

DOI:10.1002/ejic.201402930

# Pyrididine–Carboxylate Ligands as Double-Bridge Spacers in Cu<sup>I</sup> Metallacycles

Xialu Wu,<sup>[a]</sup> Wenhua Zhang,<sup>[b]</sup> Xinhai Zhang,<sup>[b]</sup> Nini Ding,<sup>\*,[b]</sup> and T. S. Andy Hor<sup>\*,[a,b]</sup>

**Keywords:** Metallacycles / N,O ligands / Crystal engineering / Macrocycles / Copper

The addition of pyridine-3-carboxylic acid (3-PyCOOH), (*E*)-3-(pyridin-3-yl)acrylic acid (3-PyCH=CHCOOH), or 3-(pyridin-4-yl)benzoic acid (3-PyPhCOOH) to the Lewis acidic [Cu(dppf)(NCMe)<sub>2</sub>][BF<sub>4</sub>] $\cdot$ 2MeCN $\cdot$ 2H<sub>2</sub>O [1 $\cdot$ 2MeCN $\cdot$ 2H<sub>2</sub>O, dppf = 1,1'-bis(diphenylphosphanyl)ferrocene] in the presence of NEt<sub>3</sub> afforded the complexes [Cu<sub>2</sub>(dppf)<sub>2</sub>(3-PyCOO)<sub>2</sub>] $\cdot$ 3CHCl<sub>3</sub> (2 $\cdot$ 3CHCl<sub>3</sub>), [Cu<sub>2</sub>(dppf)<sub>2</sub>(3-PyCH=CHCOO)<sub>2</sub>] $\cdot$ CH<sub>2</sub>Cl<sub>2</sub> $\cdot$

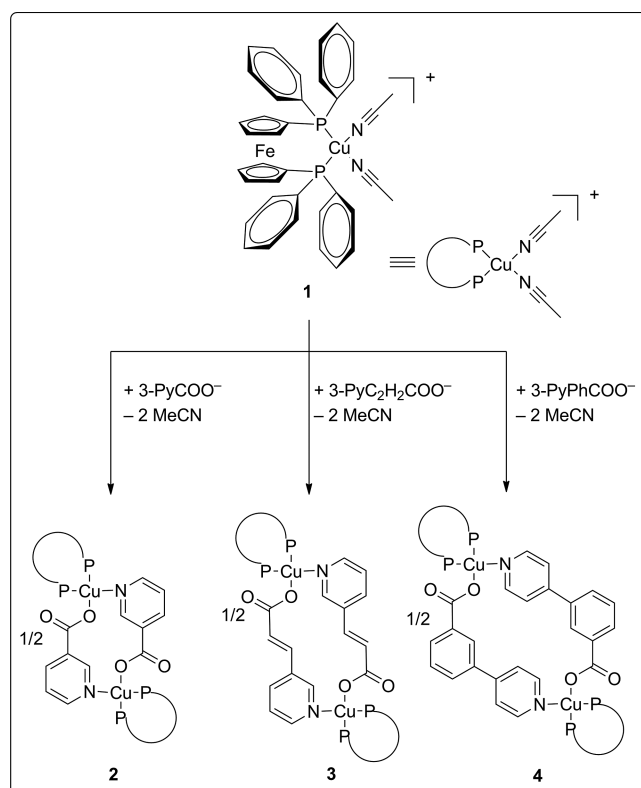
C<sub>6</sub>H<sub>14</sub> (3-CH<sub>2</sub>Cl<sub>2</sub> $\cdot$ C<sub>6</sub>H<sub>14</sub>), and [Cu<sub>2</sub>(dppf)<sub>2</sub>(3-PyPhCOO)<sub>2</sub>] $\cdot$ CH<sub>2</sub>Cl<sub>2</sub> (4 $\cdot$ CH<sub>2</sub>Cl<sub>2</sub>) with a common metallomacrocyclic core and doubly bridging pyridine–carboxylate ligands as spacers. These dinuclear complexes have been structurally characterized by single-crystal X-ray crystallography, and their emission activities have been studied.

## Introduction

Taking advantage of the abundance of spacers, numerous metal permutations, and preparative simplicity, the self-assembly of active supramolecular coordination complexes<sup>[1]</sup> provides a powerful means to create functional materials for applications in areas such as photoluminescence,<sup>[2,3]</sup> gas storage and separation,<sup>[4–7]</sup> catalysis,<sup>[8–11]</sup> and magnetism.<sup>[12,13]</sup> We are interested in hybrid spacers, such as pyridine–carboxylates, with donating sites that can be easily stereogeometrically regulated to give assemblies of defined topologies.<sup>[14–23]</sup> The synthesis of such structurally defined materials would pave the way for the creation of functional molecular materials with targeted applications.

In this paper, we report the synthesis and isolation of an electroactive Cu<sup>I</sup> precursor with two potential MeCN leaving groups to give it Lewis acidity, namely, [Cu(dppf)(NCMe)<sub>2</sub>][BF<sub>4</sub>] [1, dppf = 1,1'-bis(diphenylphosphanyl)ferrocene]. The subsequent addition reactions of 1 with pyridine-3-carboxylic acid (3-PyCOOH), (*E*)-3-(pyridin-3-yl)acrylic acid (3-PyCH=CHCOOH), and 3-(pyridin-4-yl)benzoic acid (3-PyPhCOOH) in the presence of NEt<sub>3</sub> afford three dinuclear complexes with a common cyclic central core. These assemblies from a tetrahedral [Cu(dppf)(NCMe)<sub>2</sub>]<sup>+</sup> precursor complement related assemblies of square-planar [Pt(dppf)<sub>2</sub>(NCMe)<sub>2</sub>][OTf]<sub>2</sub> (OTf<sup>−</sup> = CF<sub>3</sub>SO<sub>3</sub><sup>−</sup>)

with pyridine-3-carboxylic acid, which result in triangular topologies.<sup>[14–20,24,25]</sup> Meanwhile, some Cu<sup>II</sup> dinuclear complexes bridged by pyridine–carboxylate ligands were reported<sup>[21,22]</sup> in which N-donor ligands such as diethylenetriamine were used to end-cap the metal center in combina-



Scheme 1. Schematic representation of the syntheses of 2, 3, and 4 from 1 and the pyridine–carboxylate ligands.

[a] Department of Chemistry, Faculty of Science, National University of Singapore, 3 Science Drive 3, 117543, Singapore  
E-mail: andyhor@nus.edu.sg  
<http://staff.science.nus.edu.sg/~andyhor/>

[b] Institute of Materials Research & Engineering, 3, Research Link, 117602, Singapore

Supporting information for this article is available on the WWW under <http://dx.doi.org/10.1002/ejic.201402930>.

tion with a short pyridine–carboxylate ligand such as 3-PyCOOH as the bridging spacer. Only a small number of dinuclear complexes bridged by longer pyridine–carboxylate ligands such as 3-PyCH=CHCOOH and 3-PyPhCOOH have been reported. Therefore, we wanted to investigate if such assemblies can provide an easy route to larger functional metallomacrocycles. As part of our investigations of self-assemblies with hybrid spacers,<sup>[15,17,18,26]</sup> we decided to study the complexation of **1** with longer pyridine–carboxylate ligands.

The cationic and mononuclear  $[\text{Cu}(\text{dppf})(\text{NCMe})_2]^+$  with a chelating ligand (dppf) and two potential leaving groups is a suitable entity to form the corners in squarelike topologies.<sup>[27–31]</sup> This paper reports the self-assembly of **1** with 3-PyCOOH to give dinuclear metallacycles (Scheme 1) as the only isolated products. By a common methodology, we prepared three isostructural metallacycles. The size of their central cavities can be easily adjusted by the skeletal dimensions and configurations of the pyridine–carboxylate spacers 3-PyCOOH, 3-PyCH=CHCOOH, and 3-PyPhCOOH. The potential of the resultant ensembles as emissive materials has also been explored.

## Results and Discussion

### Syntheses and Structures of Heterometallic Dinuclear Metallacycles

The dinuclear complexes  $[\text{Cu}_2(\text{dppf})_2(3\text{-PyCOO})_2]$  (**2**),  $[\text{Cu}_2(\text{dppf})_2(3\text{-PyCH=CHCOO})_2]$  (**3**), and  $[\text{Cu}_2(\text{dppf})_2(3\text{-PyPhCOO})_2]$  (**4**) were prepared in near-quantitative yields from **1** and 3-PyCOOH, 3-PyCH=CHCOOH, and 3-PyPhCOOH in  $\text{CH}_2\text{Cl}_2$  in the presence of  $\text{Et}_3\text{N}$  at ambient temperature. The disappearance of the  $^{31}\text{P}$  NMR spectral signal at  $\delta = -12.99$  ppm of the resultant mixture indicated the exhaustion of **1**, and the sole signal for the product at ca.  $\delta = -16$  ppm suggested high product purity (Supporting Information, Figure S1).

The structures of **1** (Figure 1) and **2–4** (Figure 2) were determined by single-crystal X-ray diffraction. As shown in

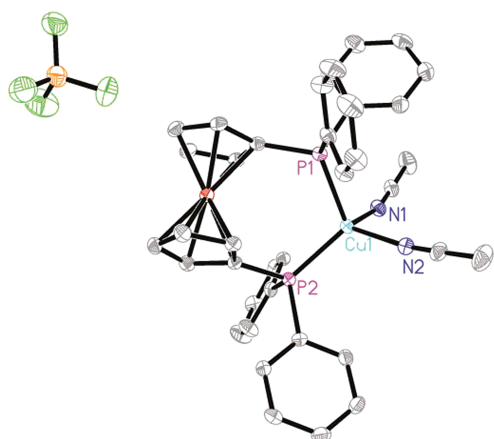


Figure 1. ORTEP drawing (50% thermal ellipsoids) of **1** (hydrogen atoms and solvent molecules are omitted).

Figure 2, the copper centers in all structures have distorted tetrahedral geometries (Tables S1–S4). Complexes **2–4** are dinuclear and isostructural with doubly bridging pyridine–carboxylate ligands coordinated through their O and N atoms. They differ only in the size of their central cavity, which is formed as a result of the cyclization of two bridging spacers over two metal centers. Complex **2** gives a 12-membered metallacycle with a diagonal distance of 6.586 Å (Cu1...Cu1A; Figure 3, top left). The introduction of a CH=CH linkage to the spacer (3-PyCH=CHCOOH) resulted in a 16-membered metallacycle with the separation extended to 9.159 Å (Figure 3, top middle). The adjustment of the cavity size by the spacer is further demonstrated when a phenyl unit is introduced to the backbone of the spacer (3-PyPhCOOH), which results in 20-membered metallacycle with a large separation of 10.006 Å (Figure 3,

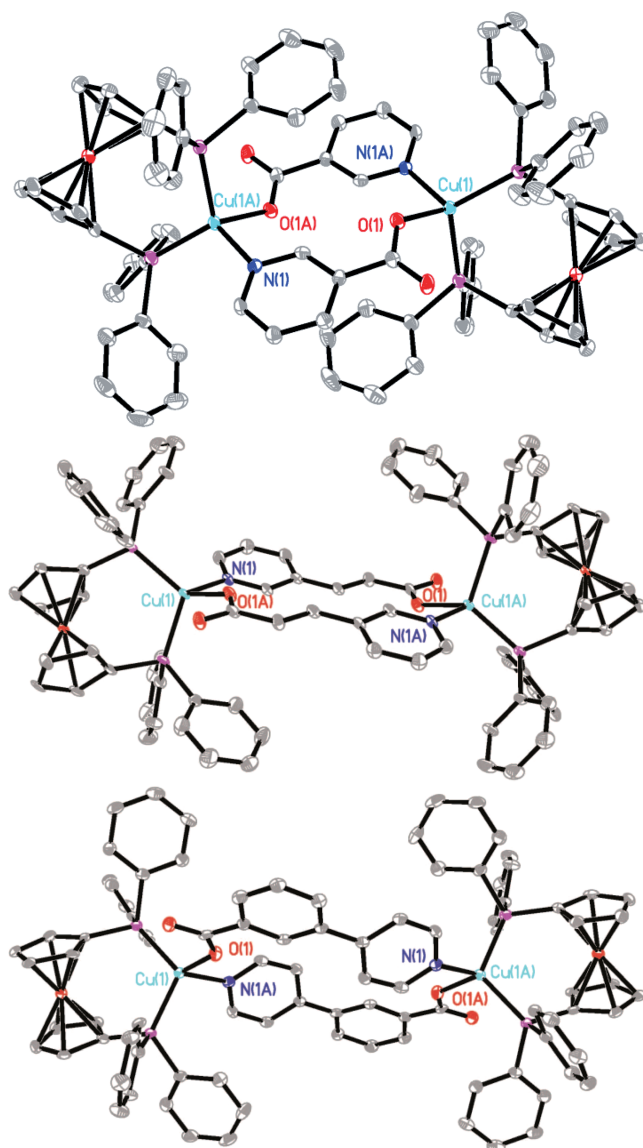


Figure 2. ORTEP drawings (50% thermal ellipsoids) of **2** (top), **3** (middle), and **4** (bottom); hydrogen atoms and solvent molecules are omitted.

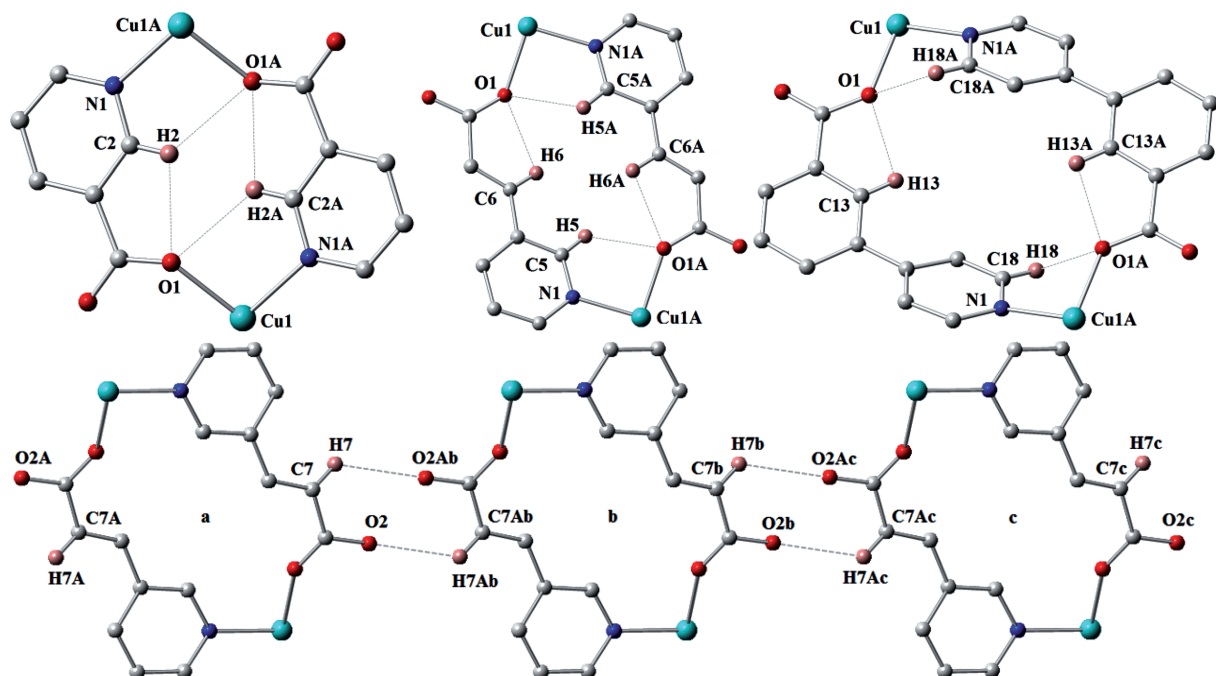


Figure 3. Secondary interactions with hydrogen bonds (shown as dashed lines) in **2** (top left), **3** (top middle and bottom), and **4** (top right).

top right). The packing patterns of **2–4** show narrow 1D solvent-free columns along the *a* axis (Figure S2).

An ESI mass spectrometry study of the three complexes in solution at ambient temperature revealed the mononuclear fragments of the metallacycles (Figure S9–S11) as [Cu(dppf)(L)] (L = 3-PyCOO<sup>−</sup>, 3-PyCH=CHCOO<sup>−</sup>, and 3-PyPhCOO<sup>−</sup>). This points to a possible mono- and dinuclear interchange in solution, as reported in related work by Shiu et al.,<sup>[23]</sup> at least under ESI-MS conditions.

Intracyclic H bonding between the C–H group and the coordinated carboxy oxygen atom is found in all three dinuclear complexes (Figure 3; the H···A of 2.37–2.55 Å and the D–H···A angles of 99–118° are summarized in Table 1). There is also secondary H bonding between neighboring cycles through a C–H group and the pendant carboxy oxygen atom in **3**, which is different from **2** and **4** (Figure 3; the H···A H-bonding distance of 2.61 Å and the D–H···A angle of 123° are shown in Table 1). These H bonds give rise to a series of interconnected cycles in the crystal packing arrangements.<sup>[23]</sup>

Table 1. Hydrogen-bonding parameters in **2**, **3**, and **4**.

	D–H···A	D–H [Å]	H···A [Å]	D···A [Å]	D–H···A [°]
<b>2</b>	C2–H2···O1	0.951	2.371	2.372	102.006
	C2–H2···O1a	0.951	2.454	3.021	118.070
<b>3</b>	C6–H6···O1	0.951	2.452	2.793	100.904
	C5–H5···O1a	0.950	2.553	3.075	114.815
	C7–H7···O2c <sup>[a]</sup>	0.950	2.616	3.240	123.546
<b>4</b>	C13–H13···O1	0.950	2.394	2.720	99.720
	C18–H18···O1a	0.950	2.539	2.992	109.339

[a] Secondary H bonding between neighboring cycles.

The emission properties of **2–4** in the solid state were investigated at various temperatures (Figures S3–S5). As

shown in Figure 4, all three dinuclear materials at 280 K show strong emissions at  $\lambda = 533, 538,$  and  $587$  nm upon excitation by 325 nm laser. The full width at half-maximum is only ca. 2 nm, which is notably much narrower than that of the reported Cu<sup>I</sup> emission (ca. 40–60 nm).<sup>[32–35]</sup> These three emission peaks can be assigned as Cu electron transfer of  $^3P_1 \rightarrow ^3F_2,$   $^3P_2 \rightarrow ^3F_4,$  and  $^3P_0 \rightarrow ^3D_3,$  respectively.<sup>[36]</sup> Control experiments on **1** and the free acids 3-PyCOOH, 3-PyC<sub>2</sub>H<sub>2</sub>COOH, and 3-PyPhCOOH under similar experimental conditions revealed that **1** showed weaker emission and the latter were nonemissive, as indicated by their poor emission spectra (Figures 4 and S6–S8). These comparisons

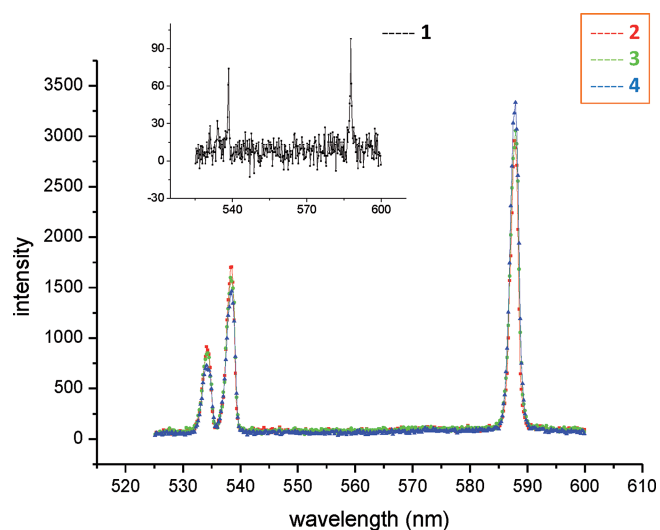


Figure 4. Emission of **2**, **3**, and **4** excited by 325 nm laser (inset: emission of **1**).

pointed to the positive optical effect of the pyridine–carboxylate ligands in these materials. Such narrow full width at half-maximum (2 nm) could point to the possible use of these materials as sharp-wavelength optical sources.

## Conclusions

We have demonstrated a simple and versatile method to construct isostructural materials with different degrees of topological cyclic features. The resultant 12-, 16-, and 20-membered metallacycles prepared from a singular self-assembly method have demonstrated the way forward for engineering functional materials directly from commercial reagents. This requires the use of a versatile Lewis acidic precursor, as evidenced by the synthesis and isolation of the solvate-coordinated complex  $[\text{Cu}(\text{dppf})(\text{NCMe})_2][\text{BF}_4]$ . The isolation of such substrates would pave the way for the creation of many other systems that demand the use of single metallic sources. The metallacycles described herein are strongly emissive at defined wavelengths. Their isolation demonstrates the possibility for the self-assembly of optically active molecular materials that can be manipulated optically through the simple choice of spacers at the synthesis level. Although such spacer-dependent emissive wavelength is not unusual, the preservation of the metallacyclic structure and nuclearity is particularly valuable. This unusual phenomenon gives a rare opportunity for the functional manipulation of molecular materials with a common or predefined structural framework. We are currently studying the extension of this methodology to related spacers and metal centers.

## Experimental Section

**General Procedures:** All reactions were performed under 99.9995% pure nitrogen by standard Schlenk techniques. All chemicals used in the synthesis were of reagent grade from commercial sources and used as received. MeCN,  $\text{CH}_2\text{Cl}_2$ ,  $\text{CHCl}_3$ , MeOH, and hexane were predried by using an MBraun MB SPS-800 solvent purification system.  $[\text{Cu}(\text{CH}_3\text{CN})_4][\text{BF}_4]$  was prepared as reported previously.<sup>[37]</sup>

All  $^1\text{H}$  [ $\delta$  (TMS) = 0.0 ppm] and  $^{31}\text{P}$  NMR spectra [ $\delta$  (85%  $\text{H}_3\text{PO}_4$ ) = 0.0 ppm] were recorded at ca. 296 K at operating frequencies of 299.96 and 121.49 MHz, respectively, with a Bruker AVANCE 300 MHz spectrometer. The elemental analyses were performed with a Perkin–Elmer PE 2400 elemental analyzer. The samples used for the elemental analyses were obtained directly from purified samples.

**$[\text{Cu}(\text{dppf})(\text{CH}_3\text{CN})_2][\text{BF}_4]$  (1):**  $[\text{Cu}(\text{CH}_3\text{CN})_4][\text{BF}_4]$  (0.66 g, 2.1 mmol) was dissolved in  $\text{CH}_3\text{CN}$  (20 mL), dppf (1.11 g, 2.0 mmol) was added, and the mixture was stirred at ambient temperature for 2 h.  $\text{Et}_2\text{O}$  (ca. 120 mL) was then added to the solution to provide a yellow precipitate of **1**, yield 1.43 g, 91%.  $^1\text{H}$  NMR ( $\text{CDCl}_3$ , 296 K):  $\delta$  = 7.43–7.50 (m, 20 H, Ph), 4.37 (s, 4 H, Cp), 4.12 (s, 4 H, Cp), 2.19 (s, 6 H,  $\text{CH}_3\text{CN}$ ) ppm.  $^{31}\text{P}$  NMR ( $\text{CDCl}_3$ , 296 K):  $\delta$  = –12.99 (s) ppm.  $\text{C}_{38}\text{H}_{34}\text{BCuF}_4\text{FeN}_2\text{P}_2$  (786.84): calcd. C 58.01, H 4.36, N 3.56; found C 58.37, H 4.30, N 3.38. ESI-MS (50 °C,  $\text{CH}_2\text{Cl}_2$ ):  $m/z$  (%) = 617.2 (100)  $[\text{Cu}(\text{dppf})]^+$ , 1186.9 (20)  $[\text{Cu}(\text{dppf})_2(\text{H}_2\text{O})]^+$ , 1270.7 (20)  $[\text{Cu}(\text{dppf})_2(\text{H}_2\text{O})(\text{OH})]^+$ .

**$[\text{Cu}_2(\text{dppf})_2(3\text{-PyCOO})_2]$  (2):** Complex **1** (78.6 mg, 0.1 mmol) was dissolved in  $\text{CH}_2\text{Cl}_2$  (25 mL), and pyridine-3-carboxylic acid (12.3 mg, 0.1 mmol) was added to give a suspension. Three drops of  $\text{Et}_3\text{N}$  were added to the suspension to immediately produce a clear solution. This solution was stirred at ambient temperature for another 30 min. The solvent and excess  $\text{Et}_3\text{N}$  were removed in vacuo to produce a pale yellow residue of **2** (64.3 mg, 87%). Further recrystallization could be carried out from a mixture of  $\text{CH}_2\text{Cl}_2$  and hexane.  $^1\text{H}$  NMR ( $\text{CDCl}_3$ , 296 K):  $\delta$  = 9.18 (s, 2 H, Py), 8.35–8.37 (d, 2 H, Py), 8.22–8.23 (d, 2 H, Py), 7.21–7.48 (m, 42 H, Ph, Py), 4.22 (s, 8 H, Cp), 4.31 (s, 8 H, Cp) ppm.  $^{31}\text{P}$  NMR ( $\text{CDCl}_3$ , 296 K):  $\delta$  = –16.026 (s) ppm. IR (KBr):  $\tilde{\nu}$  = 1607 (COO)<sub>asym</sub>, 1376, 1308 (COO)<sub>sym</sub>  $\text{cm}^{-1}$ .  $\text{C}_{82}\text{H}_{68}\text{Cl}_4\text{Cu}_2\text{Fe}_2\text{N}_2\text{O}_4\text{P}_4$  ( $2 \cdot 2\text{CH}_2\text{Cl}_2$ , 1649.94): calcd. C 59.69, H 4.15, N 1.70; found C 59.72, H 4.49, N 1.84. ESI-MS (50 °C,  $\text{CH}_2\text{Cl}_2$ ):  $m/z$  (%) = 617.2 (100)  $[\text{Cu}(\text{dppf})]^+$ , 739.4 (15)  $[\text{Cu}(\text{dppf})(3\text{-PyCOO})]^+$ , 1270.7 (25)  $[\text{Cu}(\text{dppf})_2(\text{H}_2\text{O})(\text{OH})]^+$ , 1357.8 (31)  $[\text{Cu}(\text{dppf})_2(3\text{-PyCOO})(\text{H}_2\text{O})(\text{NCMe})]^+$ .

**$[\text{Cu}_2(\text{dppf})_2(3\text{-PyCH=CHCOO})_2]$  (3):** The synthetic procedure for **3** was similar to that of **2**, except that (*E*)-3-(pyridin-3-yl)acrylic acid (14.9 mg, 0.1 mmol) was used instead of pyridine-3-carboxylic acid. Complex **3** was obtained as a yellow solid in 87% yield.  $^1\text{H}$  NMR ( $\text{CDCl}_3$ , 296 K):  $\delta$  = 9.13 (s, 2 H, Py), 8.34 (s, 2 H, Py), 8.16–8.17 (d, 2 H, Py), 7.84–7.86 (d, 2 H, Py), 7.21–7.48 (m, 42 H, Ph, CH=CH), 6.49, 6.52 (d, 2 H, CH=CH), 4.19 (s, 8 H, Cp), 4.36 (s, 8 H, Cp) ppm.  $^{31}\text{P}$  NMR ( $\text{CDCl}_3$ , 296 K):  $\delta$  = –16.213 (s) ppm. IR (KBr):  $\tilde{\nu}$  = 1605 (COO)<sub>asym</sub>, 1377, 1307 (COO)<sub>sym</sub>  $\text{cm}^{-1}$ .  $\text{C}_{86}\text{H}_{72}\text{Cl}_4\text{Cu}_2\text{Fe}_2\text{N}_2\text{O}_4\text{P}_4$  ( $3 \cdot 2\text{CH}_2\text{Cl}_2$ , 1702.02): calcd. C 60.69, H 4.26, N 1.65; found C 60.34, H 4.38, N 1.72. ESI-MS (50 °C,  $\text{CH}_2\text{Cl}_2$ ):  $m/z$  (%) = 617.2 (100)  $[\text{Cu}(\text{dppf})]^+$ , 765.6 (85)  $[\text{Cu}(\text{dppf})(3\text{-PyCH=CHCOO})]^+$ , 1270.7 (20)  $[\text{Cu}(\text{dppf})_2(\text{H}_2\text{O})(\text{OH})]^+$ , 1383.8 (100)  $[\text{Cu}(\text{dppf})_2(3\text{-PyCH=CHCOO})(\text{H}_2\text{O})(\text{NCMe})]^+$ .

**$[\text{Cu}_2(\text{dppf})_2(3\text{-PyPhCOO})_2]$  (4):** The synthetic procedure for **4** was similar to that of **2**, except that 3-(pyridin-4-yl)benzoic acid was used instead of pyridine-3-carboxylic acid. Complex **4** was obtained as a yellow solid in 90% yield.  $^1\text{H}$  NMR ( $\text{CDCl}_3$ , 296 K):  $\delta$  = 8.38 (s, 2 H, Ph of 3-PyPhCOO), 8.23–8.24 (d, 4 H, Py), 8.20–8.21 (d, 2 H, Ph of 3-PyPhCOO), 7.63–7.65 (d, 2 H, Ph of 3-PyPhCOO), 7.21–7.48 (m, 46 H, Ph, Py), 4.21 (s, 8 H, Cp), 4.33 (s, 8 H, Cp) ppm.  $^{31}\text{P}$  NMR ( $\text{CDCl}_3$ , 296 K):  $\delta$  = –16.174 (s) ppm. IR (KBr):  $\tilde{\nu}$  = 1610 (COO)<sub>asym</sub>, 1377, 1307 (COO)<sub>sym</sub>  $\text{cm}^{-1}$ .  $\text{C}_{95}\text{H}_{78}\text{Cl}_6\text{Cu}_2\text{Fe}_2\text{N}_2\text{O}_4\text{P}_4$  ( $4 \cdot 3\text{CH}_2\text{Cl}_2$ , 1887.07): calcd. C 60.47, H 4.17, N 1.48; found C 60.34, H 4.38, N 1.72. ESI-MS (50 °C,  $\text{CH}_2\text{Cl}_2$ ):  $m/z$  (%) = 617.2 (100)  $[\text{Cu}(\text{dppf})]^+$ , 815.6 (75)  $[\text{Cu}(\text{dppf})(3\text{-PyPhCOO})]^+$ , 1270.7 (95)  $[\text{Cu}(\text{dppf})_2(\text{H}_2\text{O})(\text{OH})]^+$ , 1433.8 (35)  $[\text{Cu}(\text{dppf})_2(3\text{-PyPhCOO})(\text{H}_2\text{O})(\text{NCMe})]^+$ .

**Crystal Structure Determinations:** The crystals of **1–4** were formed by the slow diffusion of hexane into solutions of the pure complexes in  $\text{CH}_2\text{Cl}_2$  or  $\text{CHCl}_3$ . The diffraction experiments were performed at 100 K with a Bruker SMART CCD diffractometer for **1**, **2**, and **4** and with a Bruker APEX II diffractometer for **3**. The instruments were both equipped with a graphite-monochromated  $\text{Mo-K}\alpha$  radiation source ( $\lambda = 0.71073 \text{ \AA}$ ). The program SMART<sup>[38]</sup> was used to collect frames of data, index reflections, and determine lattice parameters, SAINT was used to integrate the intensity of the reflections and for scaling, SADABS<sup>[39]</sup> was used for absorption correction, and SHELXTL<sup>[40,41]</sup> was used for space group and structure determination and least-squares refinements on  $F^2$ . The relevant crystallographic data and refinement details are shown in Table 2. In **1**, the asymmetric unit contains one  $\text{C}_{38}\text{H}_{34}\text{N}_2\text{P}_2\text{FeCu}$  cation, one  $\text{BF}_4$  anion, two acetonitrile molecules, and two water

Table 2. Crystallographic data and structure refinement for 1–4.

	1	2	3	4
Empirical formula	C <sub>41.50</sub> H <sub>40.25</sub> BCuF <sub>4</sub> FeN <sub>3.50</sub> O <sub>0.50</sub> P <sub>2</sub>	C <sub>80</sub> H <sub>64</sub> Cu <sub>2</sub> Fe <sub>2</sub> N <sub>2</sub> O <sub>4</sub> P <sub>4</sub>	C <sub>85</sub> H <sub>71</sub> BCl <sub>2</sub> Cu <sub>2</sub> F <sub>4</sub> Fe <sub>2</sub> N <sub>2</sub> O <sub>4</sub> P <sub>4</sub>	C <sub>92</sub> H <sub>72</sub> Cu <sub>2</sub> Fe <sub>2</sub> N <sub>2</sub> O <sub>4</sub> P <sub>4</sub>
Temperature [K]	100(2)	100(2)	123(2)	100(2)
Formula weight	864.16	1478.11	1704.81	1630.17
Space group	<i>P</i> 2 <sub>1</sub> / <i>c</i>	<i>P</i> $\bar{1}$	<i>P</i> $\bar{1}$	<i>P</i> $\bar{1}$
Crystal system	monoclinic	triclinic	monoclinic	triclinic
<i>a</i> [Å]	12.6230(11)	12.2571(11)	19.6698(15)	10.020(2)
<i>b</i> [Å]	22.748(2)	13.0080(11)	19.8141(16)	13.571(3)
<i>c</i> [Å]	13.7783(13)	17.1720(15)	20.7723(15)	14.976(3)
$\alpha$ [°]	90	69.889(2)	90	92.454(5)
$\beta$ [°]	95.899(3)	74.951(2)	112.112(2)	92.402(5)
$\gamma$ [°]	90	64.823(2)	90	92.877(5)
Volume [Å <sup>3</sup> ]	3935.5(6)	2305.9(3)	7500.3(10)	2030.0(8)
<i>Z</i>	4	1	4	1
<i>D</i> <sub>calcd</sub> [g/cm <sup>3</sup> ]	1.459	1.582	1.510	1.474
$\mu$ [mm <sup>-1</sup> ]	1.046	1.404	1.159	1.132
<i>F</i> (000)	1775	1108	3488	924
Crystal size [mm]	0.50 × 0.36 × 0.18	0.36 × 0.22 × 0.16	0.38 × 0.30 × 0.28	0.54 × 0.34 × 0.20
Index ranges	–16 ≤ <i>h</i> ≤ 15 –27 ≤ <i>k</i> ≤ 29 –17 ≤ <i>l</i> ≤ 17	–15 ≤ <i>h</i> ≤ 15 –16 ≤ <i>k</i> ≤ 16 –22 ≤ <i>l</i> ≤ 22	–24 ≤ <i>h</i> ≤ 25 –25 ≤ <i>k</i> ≤ 25 –26 ≤ <i>l</i> ≤ 23	–13 ≤ <i>h</i> ≤ 12 –17 ≤ <i>k</i> ≤ 17 –19 ≤ <i>l</i> ≤ 19
<i>R</i> <sub>1</sub> <sup>[a]</sup> , <i>wR</i> <sub>2</sub> <sup>[b]</sup> (all data)	0.0605, 0.1145	0.0842, 0.1481	0.0976, 0.1482	0.0877, 0.1501
Final <i>R</i> <sub>1</sub> , <i>wR</i> <sub>2</sub>	0.0473, 0.1084	0.0592, 0.1367	0.0624, 0.1347	0.0603, 0.1383
GOF <sup>[c]</sup>	1.042	1.034	1.064	1.035
Largest diff. peak and hole [e/Å <sup>3</sup> ]	0.706 and –0.377	1.470 and –0.865	0.898 and –1.633	1.065 and –0.989

[a]  $R_1 = \sum ||F_o| - |F_c|| / \sum |F_o|$ . [b]  $wR_2 = \{\sum w(|F_o| - |F_c|)^2 / \sum w|F_o|^2\}^{1/2}$ . [c]  $GOF = \{\sum w(|F_o| - |F_c|)^2 / (n - p)\}^{1/2}$ .

molecules. One of the acetonitrile molecules was 28% replaced by two water molecules, which makes the empirical formula C<sub>41.50</sub>H<sub>40.25</sub>BCuF<sub>4</sub>FeN<sub>3.50</sub>O<sub>0.50</sub>P<sub>2</sub>. In **3**, the hydrogen atoms of the disordered solvate molecules were not located. There is one level A alert caused by a short O2...O2 (1 - *x*, 3 - *y*, 2 - *z*) contact of 2.450 Å. The ORTEP diagrams indicated no signs of disorder for O2 or its bonded atoms. This unusual short contact is probably induced by a pair of complementary hydrogen-bonding interactions between C7–H7...O2 (1 - *x*, 3 - *y*, 2 - *z*; H7...O2 2.616 Å; ∠ C7–H7...O2 123.6°), which brings a pair of two symmetry-related O2 atoms into close proximity.

CCDC-1004474 (for **1**), -1004475 (for **2**), -1004476 (for **3**), and -1004477 (for **4**) contain the supplementary crystallographic data for this paper. These data can be obtained free of charge from The Cambridge Crystallographic Data Centre via www.ccdc.cam.ac.uk/data\_request/cif.

**Variable-Temperature Emission Study:** For the variable-temperature (VT) emission measurements, the sample was film-coated on a silica plate by slow evaporation of its CH<sub>2</sub>Cl<sub>2</sub> solution. The silica plate was then mounted on the cold finger of a closed-cycle cryostat (Janis SHI-4-5) and excited by the 325 nm line of a He–Cd laser (Kimmon KR1801C). The excitation power of the laser was 20 mW. The photoluminescent signal was dispersed through a monochromator (Acton SpectraPro 2300i) and detected with a liquid N<sub>2</sub> cooled CCD detector (Princeton, Spec-10:100).

**Supporting Information** (see footnote on the first page of this article): <sup>31</sup>P NMR spectra of **1–4**, selected bond lengths and angles of **1–4**, crystallographic packing patterns of **2–4**, variable-temperature emissions of **2–4** excited by 325 nm laser, emission of three spacers excited by a 325 nm laser, and ESI mass spectra of **2–4** showing the fragments.

## Acknowledgments

The authors acknowledge the Ministry of Education, Singapore (R-143-000-361-112), the National University of Singapore, and

the Institute of Materials Research & Engineering (IMRE) for financial support as well as Hong Yimian and Tan Geok Kheng for crystallographic assistance.

- [1] T. R. Cook, Y.-R. Zheng, P. J. Stang, *Chem. Rev.* **2013**, *113*, 734–777.
- [2] F.-J. Liu, H.-J. Hao, C.-J. Sun, X.-H. Lin, H.-P. Chen, R.-B. Huang, L.-S. Zheng, *Cryst. Growth Des.* **2012**, *12*, 2004–2012.
- [3] E. Lee, J. K. Kim, M. Lee, *Angew. Chem. Int. Ed.* **2009**, *48*, 3657–3660; *Angew. Chem.* **2009**, *121*, 3711.
- [4] M. Dinc, A. Dailly, Y. Liu, C. M. Brown, D. A. Neumann, J. R. Long, *J. Am. Chem. Soc.* **2006**, *128*, 16876–16883.
- [5] J. L. C. Rowsell, O. M. Yaghi, *J. Am. Chem. Soc.* **2006**, *128*, 1304–1315.
- [6] J.-R. Li, H.-C. Zhou, *Nat. Chem.* **2010**, *2*, 893–898.
- [7] X. S. Wang, S. Ma, P. Forster, D. Yuan, J. Eckert, J. López, B. Murphy, J. Parise, H. C. Zhou, *Angew. Chem. Int. Ed.* **2008**, *47*, 7263–7266; *Angew. Chem.* **2008**, *120*, 7373.
- [8] J. S. Seo, D. Whang, H. Lee, S. I. Jun, J. Oh, Y. J. Jeon, K. Kim, *Nature* **2000**, *404*, 982–986.
- [9] C.-D. Wu, A. Hu, L. Zhang, W. Lin, *J. Am. Chem. Soc.* **2005**, *127*, 8940–8941.
- [10] M. Fujita, Y. J. Kwon, S. Washizu, K. Ogura, *J. Am. Chem. Soc.* **1994**, *116*, 1151–1152.
- [11] M. H. Alkordi, Y. Liu, R. W. Larsen, J. F. Eubank, M. Eddaoudi, *J. Am. Chem. Soc.* **2008**, *130*, 12639–12641.
- [12] J.-P. Zhao, B.-W. Hu, X.-F. Zhang, Q. Yang, M. S. El Fallah, J. Ribas, X.-H. Bu, *Inorg. Chem.* **2010**, *49*, 11325–11332.
- [13] W. Wernsdorfer, N. Aliaga-Alcalde, D. N. Hendrickson, G. Christou, *Nature* **2002**, *416*, 406–409.
- [14] P. Teo, D. M. J. Foo, L. L. Koh, T. S. A. Hor, *Dalton Trans.* **2004**, 3389–3395.
- [15] P. Teo, L. L. Koh, T. S. A. Hor, *Chem. Commun.* **2007**, 4221–4223.
- [16] P. Teo, L. L. Koh, T. S. A. Hor, *Chem. Commun.* **2007**, 2225–2227.
- [17] P. Teo, L. L. Koh, T. S. A. Hor, *Inorg. Chem.* **2008**, *47*, 9561–9568.
- [18] P. Teo, L. L. Koh, T. S. A. Hor, *Inorg. Chem.* **2008**, *47*, 6464–6474.

- [19] P. Teo, J. Wang, L. L. Koh, T. S. A. Hor, *Dalton Trans.* **2009**, 5009–5014.
- [20] P. Teo, L. L. Koh, T. S. A. Hor, *Dalton Trans.* **2009**, 5637–5646.
- [21] C. Chen, Z.-K. Chan, C.-W. Yeh, J.-D. Chen, *Struct. Chem.* **2008**, *19*, 87–94.
- [22] F.-M. Nie, F. Lu, S.-Y. Wang, M.-Y. Jia, Z.-Y. Dong, *Inorg. Chim. Acta* **2011**, *365*, 309–317.
- [23] K.-B. Shiu, S.-A. Liu, G.-H. Lee, *Inorg. Chem.* **2010**, *49*, 9902–9908.
- [24] P. Teo, L. L. Koh, T. S. A. Hor, *Inorg. Chim. Acta* **2006**, *359*, 3435–3439.
- [25] P. Teo, L. L. Koh, T. S. A. Hor, *Inorg. Chem.* **2003**, *42*, 7290–7296.
- [26] L. Bellarosa, J. Manuel Castillo, T. Vlugt, S. Calero, N. Lopez, *Chem. Eur. J.* **2012**, *18*, 12260–12266.
- [27] S. Roy, B. Sarkar, D. Bubrin, M. Niemeyer, S. Zálíš, G. K. Lahiri, W. Kaim, *J. Am. Chem. Soc.* **2008**, *130*, 15230–15231.
- [28] H.-F. Dai, W.-Y. Yeh, *Organometallics* **2011**, *30*, 3992–3998.
- [29] J.-P. Zhang, Y.-B. Zhang, J.-B. Lin, X.-M. Chen, *Chem. Rev.* **2012**, *112*, 1001–1033.
- [30] Z. Zhang, L. Wojtas, M. Eddaoudi, M. J. Zaworotko, *J. Am. Chem. Soc.* **2013**, *135*, 5982–5985.
- [31] M. Fujita, *Chem. Soc. Rev.* **1998**, *27*, 417–425.
- [32] M. T. Miller, P. K. Gantzel, T. B. Karpishin, *J. Am. Chem. Soc.* **1999**, *121*, 4292–4293.
- [33] C. T. Cunningham, J. J. Moore, K. L. H. Cunningham, P. E. Fanwick, D. R. McMillin, *Inorg. Chem.* **2000**, *39*, 3638–3644.
- [34] A. Tsuboyama, K. Kuge, M. Furugori, S. Okada, M. Hoshino, K. Ueno, *Inorg. Chem.* **2007**, *46*, 1992–2001.
- [35] X.-L. Xin, M. Chen, Y.-b. Ai, F.-l. Yang, X.-L. Li, F. Li, *Inorg. Chem.* **2014**, *53*, 2922–2931.
- [36] J. Sugar, A. Musgrove, *J. Phys. Chem. Ref. Data* **1990**, *19*, 527–616.
- [37] X. Tang, S. Woodward, N. Krause, *Eur. J. Org. Chem.* **2009**, 2836–2844.
- [38] *SMART and SAINT Software Reference Manuals*, v. 5.611, Bruker Analytical X-ray Systems, Inc., Madison, WI, USA, **2000**.
- [39] G. M. Sheldrick, *SADABS, Program for Empirical Absorption Correction of Area Detector Data*, University of Göttingen, Germany, **1996**.
- [40] G. M. Sheldrick, *SHELX97, Programs for the Solution and Refinement of Crystal Structures*, University of Göttingen, Germany, **1997**.
- [41] G. M. Sheldrick, *Acta Crystallogr., Sect. A* **2008**, *64*, 112–122.

Received: October 8, 2014

Published Online: ■

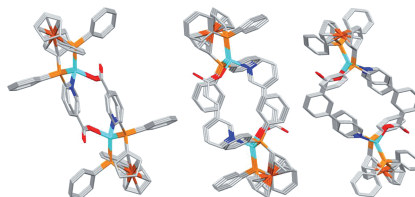
## Metallacycles

X. Wu, W. Zhang, X. Zhang, N. Ding,\*  
T. S. A. Hor\* ..... 1–7



Pyridine–Carboxylate Ligands as  
Double-Bridge Spacers in Cu<sup>I</sup> Metallacycles

**Keywords:** Metallacycles / N,O ligands /  
Crystal engineering / Macrocycles / Copper



Pyridine–carboxylate-bridged dinuclear Cu<sup>I</sup> complexes capped by 1,1'-bis(diphenylphosphanyl)ferrocene (dppf) exhibit macrocycles with diagonal distances of 6.586, 9.159, and 10.006 Å. Such cavity sizes are formed by the introduction of CH=CH or phenyl units into the original pyridine-3-carboxylic acid (3-PyCOOH) spacer.